

Study of sensor structure for measurement of magnetization characteristics in high pulsed fields

Abstract. Permanent magnets, especially Nd-Fe-B magnets are very important engineering elements that are widely used in many applications such as information, communication, acoustic and medical equipment. Detailed design of electrical and electronics equipment using permanent magnets, requires precise measurement of magnetization characteristics. It is relatively easy to obtain high field strengths in case of short pulses. However, our goal is to achieve long pulse and high fields simultaneously. Such experiment conditions imposes certain requirements on excitation coil construction (taking excitation system energy capabilities into account). Errors influencing the measurements stems from relations between tested material and pick-up sensor and excitation coil structures. This paper presents the analysis of these relations and their influence on material properties measurements accuracy and results obtained in comparison of sensors' structures.

Streszczenie. W przypadku badania magnesów często wykorzystuje się pola impulsowe. Celem pracy jest osiągniecie dostatecznie długiego impulsu o dostatecznie dużej wartości. Wymaga to odpowiedniej konstrukcji cewki magnesującej. W artykule przeanalizowano zależność między parametrami badanego materiału a parametrami, głównie dokładnością czujnika i cewki magnesującej. (Analiza struktury czujnika wykorzystywanego przy technice dużych pól impulsowych).

Keywords: high pulsed fields, magnetization characteristics, Nd-Fe-B magnet.
Słowa kluczowe: magnetyczne pola impulsowe, badanie magnesów.

Introduction

The use of permanent magnets in rotators and for various applications in information and communication, acoustics, instrumentation, and medicine continues to increase, and recently applications in automobiles and large-scale rotators such as wind power generators have been expanding as a means of achieving higher efficiency. Although precise measurements of the magnetization characteristics of the permanent magnets used is important in machine design, such measurements have not yet been made. The methods of measuring permanent magnet materials include electromagnetic excitation and pulse coil excitation [1-3].

Electromagnetic excitation has the advantages of not requiring demagnetizing field compensation and not being affected by eddy current., but it has the disadvantages of a weak generated magnetic field and abnormal attenuation of the detection signal [4]. Pulse coil excitation, on the other hand, has the advantages of easily generating a high magnetic field and no abnormal detection signal attenuation, but has the disadvantages of requiring diamagnetic field compensation for open magnetic circuits and being affected by the surface wave effect due to eddy current. Furthermore, the maximum magnetic field generated by conventional pulse coil excitation is about 10 T, which may not be sufficient to measure permanent magnet samples up to full saturation.

To perform low-frequency excitation with a pulsed excitation device requires a higher magnetization coil winding count and increased inductance. In that case, however, resistance also increases, so a high magnetic field cannot be created. To overcome that problem, liquid nitrogen can be used to lower the resistance of the magnetization coil by cooling, thus enabling a high magnetic field from low-frequency pulsed excitation.

Measurement of magnetization characteristics with a high pulsed magnetic field is done mainly by induction. The inductive method involves inserting the sample to be measured into a magnetization detection coil, applying a high pulsed magnetic field, and calculating the magnetization characteristics from the measured voltage induced in a detection coil. The three main types of magnetization detection coil are the series type, the parallel type, and the coaxial [5]. In this paper, we exclude the

parallel type from study because the bore diameter of the magnetization coil is large, and report on a comparison of the series type and coaxial type magnetization detection coils.

Power source for pulses

We designed and assembled a pulsed power supply magnetizer for performing low-frequency pulsed excitation with a high magnetic field. The magnetizer circuit diagram is presented in Fig. 1. The fabricated system is equipped with 14 2000 μ F, 3,000 V capacitors and 10 10,000 μ F, 1000 V capacitors, which respectively store 126 kJ and 50 kJ of energy. The capacitors are charged via a rectifier, with the circuit selected by electromagnetic contacts. The discharge control employs a high-power thyristor, the input signal of which is controlled by using an optical fiber for switching the thyristor on and off, which provides electrical isolation for safety. The discharge current is a damped oscillation under normal conditions, so a reverse voltage relative to the charging voltage is applied to the capacitor. Because the reverse voltage reduces the life of the capacitor, a crowbar circuit is included to prevent that. The crowbar circuit also extends the pulse rise time. Inserting a circuit that enables output of a damped oscillation waveform makes it possible to demagnetize a magnetized sample, etc. The direction of the generated magnetic field can be changed with a polarity selection switch, allowing measurement of the hysteresis curve of the sample.

Magnetization coil

Pulsed excitation of the measurement sample requires a magnetization coil. A short-pulsed magnetic field can be used to easily generate a relatively high magnetic field, but because an eddy current flows in the measurement sample, accurate measurement of the magnetization characteristics is not possible. For that reason, it is necessary to generate a long-pulsed magnetic field, which requires a magnetization coil that has a large inductance. The inductance increases in proportion to the square of the number of turns of winding, but increasing the winding count also increases the resistance of the magnetization coil and thus reduces current flow. The result is a weaker magnetic field.

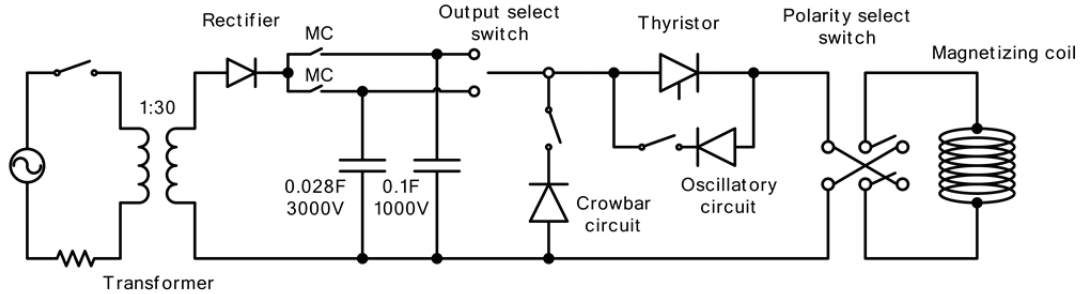


Fig. 1 Circuit of magnetizer.

Measurement of the magnetization characteristics of magnetic materials up to the saturation region in the hard magnetization direction, particularly for sintered rare-earth magnets, requires generation of a high magnetic field of at least 10 T. Generation of the high magnetic field and long-pulse waveform needed for that requires a reduction in the resistance of the magnetization coil. Because the resistance depends on temperature, cooling the magnetization coil can lower the resistance. We therefore used liquid nitrogen to cool the magnetization coil. The change in resistance as the temperature changes is described by the following equation.

$$(1) \quad R_T = R_{RT} \{ 1 + \alpha(T - T_{RT}) \}$$

here, R_{RT} is the resistance at room temperature, α is the temperature coefficient of resistance, and T_{RT} is room temperature. The fabricated magnetization coil has an inside diameter of 15 mm, length of 200 mm, and winding count of 1500 turns. The resistance at room temperature is 1.32Ω . The resistance when liquid nitrogen is used is 0.20Ω according to Eq. (1). The temperature coefficient of copper wire is 3.85×10^{-3} , with room temperature taken as 25 deg C and the temperature of liquid nitrogen as -196 deg C. The actual measured value, 0.20Ω , matches the theoretical value. This measurement result shows that using liquid nitrogen can lower the magnetization coil resistance to about 1/6 the room temperature value. A comparison of generated magnetic field showing the effect of the liquid nitrogen cooling is presented in Fig. 2. We see from the figure that the liquid nitrogen cooling increases the generated magnetic field by a factor of three.

Types of magnetization detection coils

Magnetization detection coils are coming into wide use for measuring the magnetization characteristics of permanent magnets by means of pulsed magnetic fields. When measuring magnetization by the induction method, two coils of opposite directions are connected in series so that no voltage is induced in the detection coil by a changing external magnetic field when no sample is present. The three basic forms of detection coils are shown in Fig. 3. In the work reported here, the parallel type was excluded from study because the large diameter of the magnetization coil bore results in a weak magnetic field. The investigation was limited to the series and coaxial types of detection coils.

Series type magnetization detection coil

Figure 3 (a) illustrates the series type magnetization detection coil. The coil in the middle is the magnetic flux density detection coil; the coils above and below it are cancelling coils. Denote the sample cross-sectional area as $S_s [m^2]$, the cross-sectional area of coils A and B as $S_C [m^2]$, the winding count as N_1 , the cross-sectional area of coil C as

$S_C [m^2]$, and the winding count of coil C as N_2 . The relation between winding counts N_1 and N_2 is $N_2 = 2N_1$.

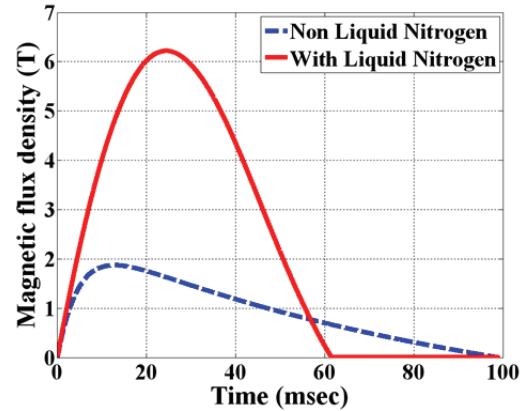


Fig. 2 Influence of magnetization coil's temperature on pulse-field amplitude.

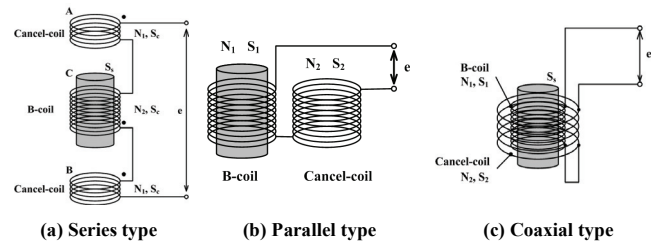


Fig. 3 Various types of magnetization detection coils.

Denoting the magnetic field as H and the sample magnetization per unit volume as M , the respective coil magnetic flux density and magnetic flux are given by the following equations.

$$(2) \quad B_A = B_B = \mu_0 H$$

$$(3) \quad B_C = \mu_0(H + M)$$

$$(4) \quad \phi_A = \phi_B = S_C \mu_0 H$$

$$(5) \quad \phi_C = S_C \mu_0 H + S_S \mu_0 M$$

The voltage induced in the series type detection coil is expressed by the following equation.

$$(6) \quad e = -N_2 \frac{d\phi_c}{dt} + \left(N_1 \frac{d\phi_A}{dt} + N_1 \frac{d\phi_B}{dt} \right) \\ = - \left(N_2 S_C \mu_0 \frac{dH}{dt} + N_2 S_S \mu_0 \frac{dM}{dt} \right) + 2N_1 S_C \mu_0 \frac{dH}{dt} \\ = -N_2 S_S \mu_0 \frac{dM}{dt}$$

The induced voltage includes the time differential of the magnetization M , dM/dt , so M can be obtained by integrating the induced voltage as in the following equation.

$$(7) \quad M(t) = -\frac{1}{\mu_0 N_2 S_S} \int e(t) dt$$

Coaxial magnetization detection coil

The coaxial magnetization detection coil is shown in Fig. 3 (c). The inside coil is for detecting magnetic flux density and the outside coil is the cancelling coil. We denote the sample cross-sectional area as S_S [m^2], the inside coil cross-sectional area as S_1 [m^2], the winding count as N_1 , the outside coil cross-sectional area as S_2 [m^2], and the winding count as N_2 . The area-turn relation of the coils is $N_1 S_1 = N_2 S_2$. The respective coil magnetic flux density and magnetic flux are given by the following equations.

$$(8) \quad B_1 = B_2 = \mu_0(H + M)$$

$$(9) \quad \phi_1 = S_1 \mu_0 H + S_S \mu_0 M$$

$$(10) \quad \phi_2 = S_2 \mu_0 H + S_S \mu_0 M$$

The induced voltage of the coaxial magnetization detection coil is expressed as the following equation.

$$(11) \quad \begin{aligned} e &= -N_1 \frac{d\phi_1}{dt} + N_2 \frac{d\phi_2}{dt} \\ &= (N_1 S_1 - N_2 S_2) \mu_0 \frac{dH}{dt} - (N_1 - N_2) S_S \mu_0 \frac{dM}{dt} \\ &= -(N_1 - N_2) S_S \mu_0 \frac{dM}{dt} \end{aligned}$$

The magnetization M can be obtained by integrating the induced voltage in the same way as for the series type magnetization detection coil with the following equation.

$$(12) \quad M(t) = -\frac{1}{\mu_0 (N_1 - N_2) S_S} \int e(t) dt$$

Measurement system

The block diagram of the measurement system is shown in Fig. 4. The sample is inserted into the middle of the magnetization characteristics and magnetic field strength detection coil, which is then inserted into the magnetization coil. The magnetization coil is sufficiently cooled with liquid nitrogen and then the capacitor is charged. Next, a discharge signal is output to discharge the capacitor and generate a pulsed magnetic field.

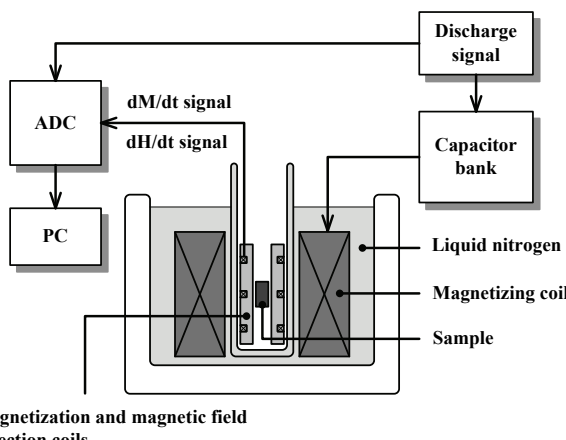


Fig. 4 Block schematic of magnetization characteristics measurement system.

The signal output by the sensor that detects the magnetization characteristics is input to the ADC, which is triggered by the discharge signal. The measured output signal is numerically integrated by a personal computer to obtain the magnetization characteristics of the sample. The ADC is a National Instrument device with a 24-bit resolution and a sampling rate of 2 MS/s.

Verifying magnetization detection coil accuracy

To test the measurement accuracies of the magnetization detection coils, we used highly-pure Ni, Co, and Fe reference samples. The reference samples are 99.99% pure and have a diameter of 10 mm and a length of 20 mm. The saturation magnetization of pure Ni, Co, and Fe were first obtained [6] and the measurement results for the series and coaxial magnetization detection coils were compared (Fig. 5, 6 and 7).

In Fig. 8, the measured values are compared with the theoretical values; in Fig. 9, the magnetization detection coil error relative to the theoretical values is shown. These results show that the series type sensor has the lowest measured magnetization for all samples, with an error relative to the theoretical value of 15 %. The error is believed to be introduced by the difference in the magnetic field component $\mu_0 H$ of the cancelling coils that are positioned above and below the measurement sample in the series type magnetization detection coil, which affects the sample. The coaxial magnetization detection coil has two coils placed in a coaxial configuration, so the difference in magnetic field component $\mu_0 H$ is small, so more accurate measurement is possible. These results show that the coaxial type of magnetization detection coil should be used for measuring magnetization characteristics with a pulsed magnetic field.

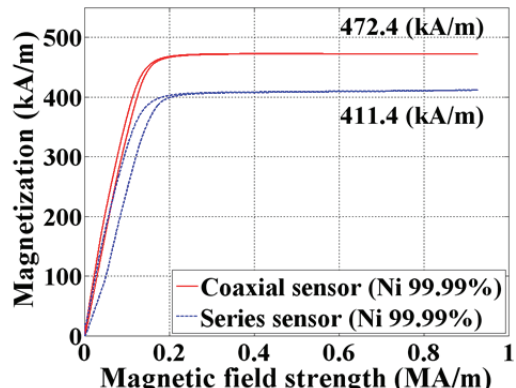


Fig. 5 Comparison of M-H curves of Ni sample for different detection coils.

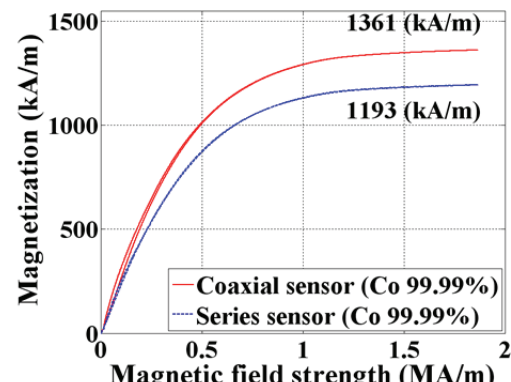


Fig. 6 Comparison of M-H curves of Co sample for different detection coils.

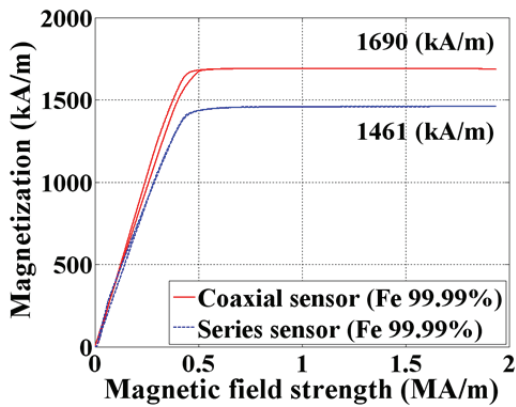


Fig. 7 Comparison of M-H curves of Fe sample for different detection coils.

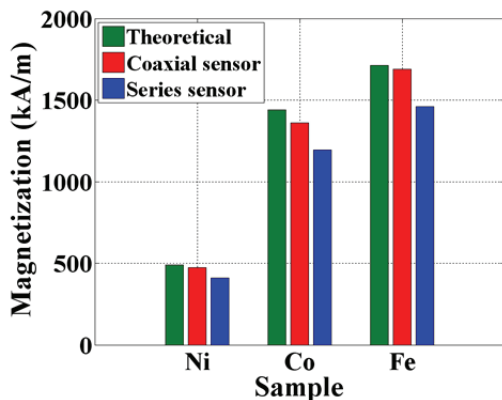


Fig. 8 Comparison of magnetization value.

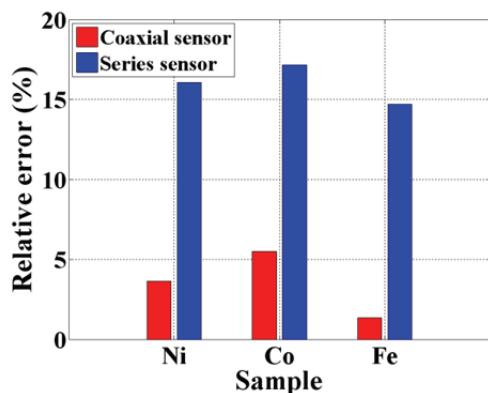


Fig. 9 Relative error of detection coils.

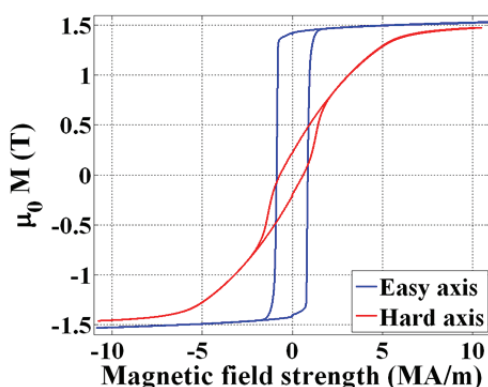


Fig. 10 M-H curves of Nd-Fe-B magnets in high magnetic fields.

Measuring characteristics of sintered Nd-Fe-B magnets in high magnetic fields

We measured the magnetization characteristics of sintered Nd-Fe-B magnets using a high magnetic field. The cylindrical samples were 20 mm long and 10 mm in diameter. The measurements were done on samples that were cut in the easy magnetization direction and in the difficult magnetization direction. To measure the magnetization characteristics in the easy and hard magnetization directions, we applied a 17-T magnetic field. As we see from the results presented in Fig. 10, the fabricated measurement system can measure the magnetization characteristics of a sintered Nd-Fe-B magnet up to the saturation region for both directions.

Conclusion

For more accurate measurement of the magnetization characteristics of magnetic materials, we constructed a magnetizer system and magnetization coil to investigate the measurement accuracy of series and coaxial types of detection coils. The results show that the coaxial coil is capable of the most accurate measurement. Because this system can be used to measure the magnetization characteristics of various magnetic materials in a high magnetic field, it will be very useful in determining the magnetization characteristics of magnetic materials.

REFERENCES

- [1] S. Chikazumi, *Physics of Ferromagnetism*, Second Edition, Clarendon Press, Oxford, 1997
- [2] F. Herlach and N. Miura, *High Magnetic Fields, Science and Technology*, Vol.1-3, World Scientific, 2003-2006
- [3] H. Knoepfel, *Pulsed High Magnetic Fields*, North-Holland Publishing Co., 1970
- [4] Subcommittee on High-performance Magnets and their Applications, *High-performance Magnet Thermal Stability, Applications and Coercive Force*, IEEJ Technical Reports No. 1149, 2009
- [5] T. Sakakibara, H. Mitamura, T. Tayama and H. Amitsuka, *Jpn. J. Appl. Phys.*, 33, 1994, 5067
- [6] National Astronomical Observatory of Japan, *Chronological Scientific Tables*, Maruzen, 2009

Authors: Mr. Yasushi Nakahata, Regional Technological Collaboration Promotion Bureau, Oita Prefectural Organization for Creation Industry, 1-4361-10 Takaenishi, 870-1117, Oita, E-mail: y.nakahata@oita-mag.jp; dr. Bartosz Edmund Borkowski, Regional Technological Collaboration Promotion Bureau, Oita Prefectural Organization for Creation Industry, 1-43610-10 Takaenishi, 870-1117, Oita, E-mail: b.borkowski@oita-mag.jp; dr. Hiroyasu Shimoji, Regional Technological Collaboration Promotion Bureau, Oita Prefectural Organization for Creation Industry, 1-4361-10 Takaenishi, 870-1117, Oita, E-mail: simoji@oita-mag.jp; prof. Koji Yamada, Open Innovation Center, Saitama University, 255 Shimo-ohkubo, Sakura-ku, Saitama City, 338-8570, Saitama, E-mail: yamasan@fms.saitama-u.ac.jp; prof. Takashi Todaka, Department of Electrical and Electronic Engineering, Faculty of Engineering, Oita University, 700 Dannoharu, 870-1192, Oita, E-mail: todaka@cc.oita-u.ac.jp; prof. Masato Enokizono, Department of Electrical and Electronic Engineering, Faculty of Engineering, Oita University, 700 Dannoharu, 870-1192, Oita, E-mail: enoki@cc.oita-u.ac.jp